

MICRONIZATION OF FLUFENAMIC ACID WITH RAPID EXPANSION OF SUPERCRITICAL SOLUTION (RESS) METHOD

Cheng-Chou Tsai, Ming-Jer Lee, Ho-mu Lin*

*Department of Chemical Engineering, National Taiwan University of Science and Technology,
43 Keelung Road, Section 4, Taipei 106-07, Taiwan*

E-mail address: hml@ch.ntust.edu.tw (H. M. Lin); Fax: +886-2-2737-6644

Abstract

Ultra-fine particles of flufenamic acid (FFA, a fluorinated and non-steroidal anti-inflammatory drug) were prepared with a novel rapid expansion of supercritical solution (RESS) technique. The influence of various process variables on the morphology and the mean size of the resultant particles were investigated experimentally. These process variables include extraction temperature (40 and 60°C), extraction pressure (11-21 MPa), pre-expansion temperature (115-135°C), crystallization temperature (30-60°C), inside diameter of capillary tube (25 and 50 μm), length of capillary tube (50 and 100 mm), and spraying distance (10 and 20 mm). The particle size of the pharmaceutical substance was significantly reduced after the RESS processing. Among the investigated parameters, the extraction temperature and spraying distance were found to be minor factors over the operating conditions. While sticky agglomerates were obtained from lower extraction pressures with larger and/or longer capillary tube, needle-like crystals were produced at higher extraction pressures with smaller and/or shorter capillary tube. Moreover, operating at lower pre-expansion temperatures and higher crystallization temperatures yielded larger size of needle-like crystals. The polymorphism of FFA converted from the original Form I into the Form III after the RESS processing. The results of this study provided us valuable experimental evidences to manipulate the morphology and the mean size of flufenamic acid particulate products through the RESS process.

1. Introduction

Increasing the bioavailability of drugs can be achieved through size reduction techniques. However, the conventional micronization processes, such as milling, lyophilization, grinding, granulation, salting out, and spray-drying, suffer from several drawbacks including thermal and chemical degradations, large particle size, broad particle size distribution, solvent residues, etc. Moreover, the release of heat and the presence of solvent may induce the conversion of drug's polymorphism and thus may affect its therapeutic efficacy. It is essentially needed to development of alternative micronization methods for producing sufficiently small and solvent-free particles with uniform size distribution and without the risk of degradation. Among several others, the rapid expansion of supercritical solution (RESS) technique is one of novel methods to meet the requirements

as mentioned above. In the present study, ultra-fine particles of flufenamic acid (FFA), a fluorinated and non-steroidal anti-inflammatory drug, were prepared by the RESS technique. The influence of various process variables on the morphology and the mean size of the resultant particles was investigated experimentally. The polymorphism of the original FFA and a representative RESS processed sample were characterized by Fourier transform infrared spectrometer (FTIR) and differential scanning calorimeter (DSC).

2. Experimental method

2.1. Materials and analytical methods

Flufenamic acid (FFA, 97+ %) was purchased from Sigma-Aldrich (USA). Carbon dioxide (99.5+ %) was supplied by Liu-Hsiang Gas Co. (Taiwan). Ethanol (95 %), for cleaning only, was purchased from Shimakyu Chemical (Japan). All the chemicals were used without further purification.

2.2. Apparatus and procedure

Fig. 1 illustrates the schematic diagram of the RESS apparatus, which consists of three main units: extraction, pre-expansion, and precipitation. Its operating procedure is described as follows. Carbon dioxide was cooled and then pressurized to a pre-specified pressure by a high-pressure liquid pump (**4**, Minipump, operable up to 40 MPa, LCD Milton Roy, USA). At the initial stage of each run, carbon dioxide flowed through the bypass line (lower part) of the extraction unit and continuously passed through the pre-expansion unit for 1-2 hours to built-up the desired operating pressure. After that, carbon dioxide flow was switched to the extraction cell (**8**), which comprises two stainless steel tubes (0.359" I.D. and 10" length of each, Autoclave Engineers, USA) in series. Dried raw FFA particles have been blended with glass beads and packed into the extraction cell in several sections separated with glass wool. A glass wool plug was placed at the top (outlet) of the extraction cell to prevent entrainment of FFA. The pre-heaters (**7**) and the extraction cell were submerged in a thermostatic bath (**6**) and controlled to within ± 0.1 K. A precision thermometer (**9**, Model 1560, Hart Scientific, USA) with a platinum resistance temperature detector (RTD) probe was employed to measure the extraction temperature with an uncertainty of ± 0.02 K. Pressure in the extraction cells were measured by a pressure transducer (**10**, PDCR-4070, 0-35 MPa, Druck, UK) equipped with a digital indicator (DPI-280, Druck, UK) accurate to ± 0.1 %.

The gas stream leaving the extraction cell was diverted to the pre-expansion unit, where was wrapped with heating tapes (**11**) and well insulated. The temperature in the pre-expansion unit (T_{pre}) was monitored at the top of capillary tube (**12**) by a RTD probe (**9**) with an uncertainty of ± 0.2 K. The temperature of pre-expansion unit was regulated to within ± 0.5 K.

The high-pressure gas stream was then depressurized to atmospheric pressure in expansion chamber (**13**) through the capillary tube (1/16", O.D., PEEK, 50 or 100 mm long \times 0.025 or 0.05 mm O.D.). The capillary tube was also heated to avoid solid deposition during rapid expansion of the gas stream. A glass slide was placed below the tip of the capillary tube to collect the precipitated FFA particles. Temperature of the precipitation unit (T_{cry}) was controlled by a thermostatic circulator

(RTE-221, Neslab, USA) with a stability of ± 0.1 K. An ethanol solvent reservoir (**15**) was used for removal of FFA left in the pre-expansion unit at the end of each run. The total volume of carbon dioxide was measured by a wet test meter (**14**, Alexander Wright Inc., UK), accurate to ± 0.25 %.

2.3 Characterization

A high resolution field-emission scanning electron microscope (FESEM; JSM-6500F, JEOL, Japan) was used to characterize the size and shape of the precipitated FFA particles. Each particulate sample was platinum-coated by a sputter (JFC-1300, JEOL, Japan) prior to FESEM analysis. The SigmaScan Pro 5 software was used to determine the mean size and the particle size distribution (PSD) of the particulate samples. At least 200-300 particles were counted from FESEM images to calculate the mean size and the PSD. FTIR (FTS-3500, Bio-Rad, USA) and DSC (Jade DSC, Perkin Elmer, USA) were utilized to characterize the polymorphism of the raw FFA and the FFA samples after the RESS processing.

3. Results and discussion

3.1 Effects of extraction pressure, extraction temperature and spraying distance

Table 1 lists the RESS experimental conditions. The raw FFA exhibits irregular shape with broad PSD as shown in Fig. 2. The FESEM images of four FFA samples after the RESS processing are illustrated in Fig. 3. As the extraction pressures were changed from 11 to 21 MPa, the morphologies of FFA particles varied from sticky agglomerates to needle-like crystals as presented in Figs. 3(a), 3(b), 3(c) and 3(d). As shown in Fig. 3(d), the particle size of the sample of run #9, for example, distributes from 1 to 5 μm and from 0.1 to 0.7 μm for the lengths of major and minor axes, respectively. It is indicated that ultra-fine micro-metric FFA particles with narrow PSD can be produced by the RESS process. Additionally, the influence of both extraction temperature and spraying distance on the mean size and PSD of the particulate samples are rather minor over entire range of experimental conditions.

3.2 Effects of pre-expansion temperature and crystallization temperature

The FESEM images in Figs. 4 and 5 illustrate the effects of the pre-expansion temperature and the crystallization temperature on the characteristics of FFA particulate samples, respectively. Operating at lower pre-expansion temperature and higher crystallization temperature yield relatively longer and thinner needle-like crystals, whose mean lengths of major and minor axes are about 2.5 and 0.5 μm , respectively. Again, Fig. 6 shows the RESS treatment can effectively reduce the particle size and narrow the PSD for FFA.

3.3 Effects of inside diameter and length of capillary tube

Both inside diameter and length of capillary tube were found to affect the morphology of the resultant FFA particles. Irregular fused flats were produced by using larger capillary tube as illustrated in Fig. 7 (a), while rectangular-like agglomerates were generated by using longer capillary tube as shown in Fig. 7 (b).

3.4 Characterization of polymorphism from FTIR and DSC

An important infrared spectral feature to distinguish the different crystal forms of the flufenamic acid is the NH stretching band¹. The NH stretching band is at 3321–3322 cm⁻¹ for polymorph I and 3315–3316 cm⁻¹ for polymorph III of FFA. Fig. 8 illustrates that the particles of raw FFA and those after the RESS processed are characterized as polymorph I and polymorph III, respectively. Fig. 9 shows that the DSC thermogram (b), from the RESS processed FFA particles, has two endothermic peaks at 126°C and 134°C which are corresponding to the melting of Form III and Form I^{2,3}, respectively. As evidenced from the FTIR and the DSC observations, the polymorphism of FFA particles has been changed before and after the RESS processing.

4. Conclusions

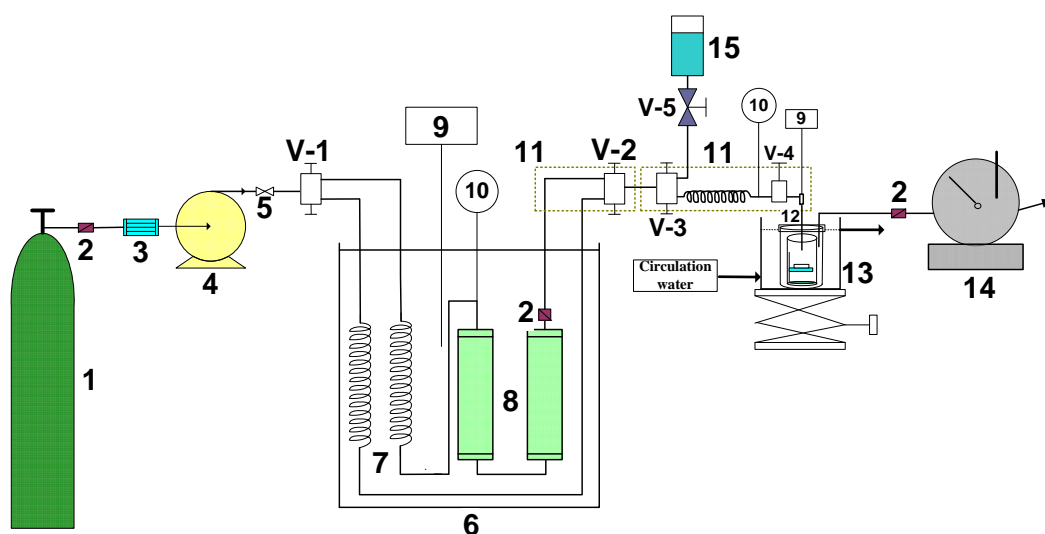
The RESS process was successfully applied to produce ultra-fine FFA particles with narrow size distribution. The mean particle size can be reduced down to submicron and micron scales and different morphologies can be obtained from the RESS processing with different process conditions. Extraction pressure, pre-expansion temperature, crystallization temperature, and dimension of capillary tube were found to be major factors of the RESS process. Operating at lower pre-expansion temperature and higher crystallization temperature yielded longer and thinner needle-like crystals. According to the analysis results from the FTIR and the DSC, the polymorphism of FFA particles converted from the original Form I into Form III after the RESS processed.

References

- (1) Gilpin, R.K.; Zhou, W., “Infrared Studies of the Polymorphic States of the Fenamates,” *J. Pharm. Biomed. Anal.*, 37, 509~515 (2005).
- (2) Romero, S.; Bustamante, P.; Escalera, B.; Cirri, M.; Mura, P., “Characterization of the Solid Phases of Paracetamol and Fenamates at Equilibrium in Saturated Solutions,” *J. Therm. Anal. Cal.*, 77, 541~554 (2004).
- (3) Threlfall, T.L., “Analysis of Organic Polymorphys,” *Analyst*, 120, 2435~2460 (1995).

Table 1. The RESS experimental conditions

Run #	Factors						
	T_{ext} (°C)	P_{ext} (MPa)	T_{pre} (°C)	T_{cry} (°C)	D_{nozzle} (μm)	L_{nozzle} (mm)	Z (mm)
1	40	21	125	45	25	50	10
2	60	11	125	45	25	50	10
3	60	13	125	45	25	50	10
4	60	15	125	45	25	50	10
5	60	21	115	60	25	50	10
6	60	21	125	60	25	50	10
7	60	21	135	60	25	50	10
8	60	21	125	30	25	50	10
9	60	21	125	45	25	50	10
10	60	21	125	45	50	50	10
11	60	21	125	45	25	100	10
12	60	21	125	45	25	50	20



- | | | |
|--|-------------------------|-----------------------|
| 1. CO ₂ cylinder | 6. Thermostatic bath | 11. Heating tape |
| 2. Filter | 7. Pre-heater | 12. Capillary tube |
| 3. Cooler | 8. Equilibrium cell | 13. Expansion chamber |
| 4. Liquid pump | 9. Thermometer | 14. Wet test meter |
| 5. Check valve | 10. Pressure transducer | 15. Solvent reservoir |
| V-1, V-2, V-3, V-4, V-5: Needle valves | | |

Fig. 1. Schematic diagram of the RESS apparatus.

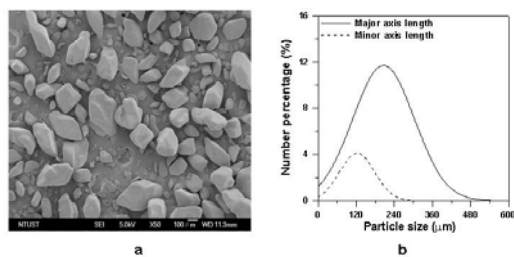


Fig. 2. (a) FESEM image of raw FFA particles (b) particle size distribution of raw FFA.

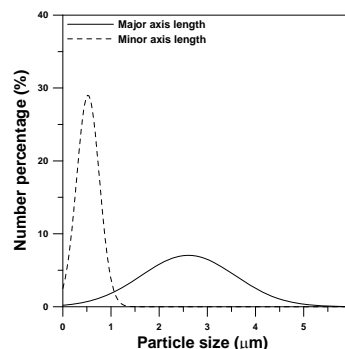


Fig. 6. Particle size distribution of RESS processed FFA; run #5.

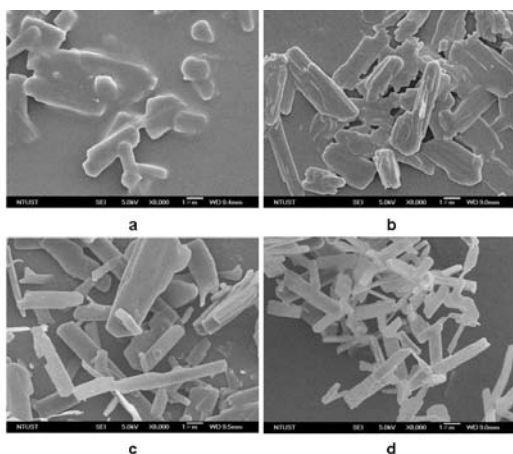


Fig. 3. FESEM images of FFA particles (a) $P_{ext} = 11$ MPa, run #2 (b) $P_{ext} = 13$ MPa, run #3 (c) $P_{ext} = 15$ MPa, run #4 (d) $P_{ext} = 21$ MPa, run #9.

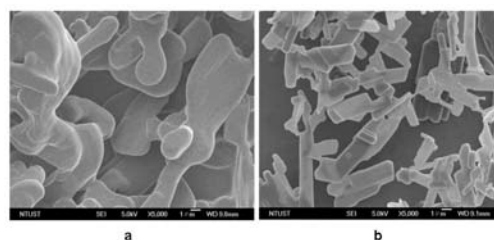


Fig. 7. FESEM images of FFA particles (a) $D_{nozzle} = 50$ μm, run #10 (b) $L_{nozzle} = 100$ mm, run #11.

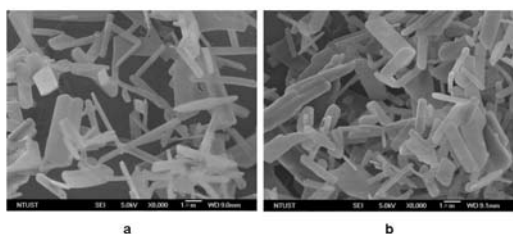


Fig. 4. FESEM images of FFA particles (a) $T_{pre} = 115^{\circ}\text{C}$, run #5 (b) $T_{pre} = 135^{\circ}\text{C}$, run #7.

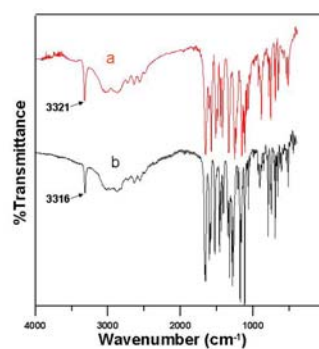


Fig. 8. FTIR spectrum of (a) raw FFA, (b) RESS processed FFA; run #9.

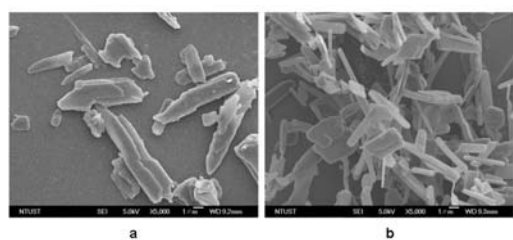


Fig. 5. FESEM images of FFA particles (a) $T_{cry} = 30^{\circ}\text{C}$, run #8 (b) $T_{cry} = 60^{\circ}\text{C}$, run #6.

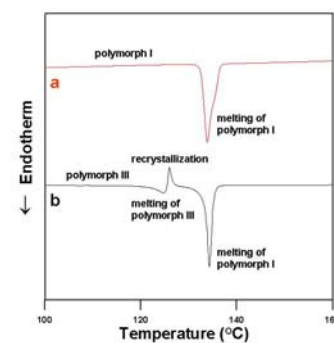


Fig. 9. DSC thermograms of (a) raw FFA, (b) RESS processed FFA; run #9.